Multifunctionality of V-type ATPase during asexual growth and development of *Plasmodium falciparum*

Neeta Shadija[1], Swati Dass[1], Wei Xu[1], Hangjun Ke[1]

[1] Center for Molecular Parasitology, Department of Microbiology and Immunology, Drexel University College of Medicine, Philadelphia, Pennsylvania, USA, 19129

Correspondence, hk84@drexel.edu

Abstract

V-type ATPases are highly conserved hetero-multi-subunit proton pumping machineries found in all eukaryotic organisms. They use ATP hydrolysis to pump protons, acidifying intracellular or extracellular compartments, and are thus crucial for various biological processes. Despite being evolutionarily conserved in malaria parasites, this proton pump remains understudied. To understand the localization and biological function of V-type ATPase in the deadliest human malaria parasite *Plasmodium falciparum*, we utilized CRISPR/Cas9 to endogenously tag the subunit A of the V_1 domain at the C-terminus. V_1A (PF3D7_1311900) was tagged with a triple hemagglutinin (3HA) epitope and TetR-DOZI-aptamers for conditional expression under the regulation of anhydrotetracycline. Through immunofluorescence assays, we identified that V-type ATPase was expressed throughout the intraerythrocytic developmental cycle and was mainly localized on the digestive vacuole and plasma membrane. Immuno-electron microscopy further revealed that V-type ATPase was also localized on secretory organelles, such as rhoptries in merozoites. Knockdown of V_1A led to cytosolic pH imbalance and blockage of hemoglobin digestion in the digestive vacuole, resulting in an arrest of parasite development in the trophozoite stage and, ultimately, parasite demise. Using BN-PAGE/Western blot, we detected a large molecular weight complex (~ 1.0 MDa) corresponding to the total molecular weights of V_1 and V_o domains. The complex was readily disrupted by the V-type ATPase specific inhibitor Bafilomycin A1, but not by low glucose conditions or treatment with chloroquine. Together, our data suggest that V-type ATPase is localized on several subcellular compartments in *P. falciparum* and plays critical roles to support malaria parasites to grow and replicate inside red blood cells.

Introduction

Malaria remains one of the deadliest infectious diseases worldwide. In 2021, the WHO reported 247,000,000 malaria cases and 619, 000 deaths[1]. The causative agent of this disease is the protozoan parasite called *Plasmodium*, belonging to the phylum Apicomplexa. Among the five *Plasmodium* species infecting humans (*P. falciparum*, *P. vivax*, *P. ovale*, *P. malariae*, *P. knowlesi*), *P. falciparum* is responsible for the majority of malaria cases and deaths worldwide. All clinical symptoms of malaria arise due to the repetitive growth of the parasites in red blood cells (RBCs); hence, the intraerythrocytic developmental cycle (IDC) or the asexual blood stage has long been recognized as a crucial target for developing antimalarial interventions.

Throughout the IDC, malaria parasites reside in a parasitophorous vacuole and contain many intracellular compartments, including the cytosol, the digestive vacuole (DV) for hemoglobin digestion, the nucleus/ER/Golgi apparatus, the mitochondrion, the apicoplast, and secretory organelles in merozoites. Some of these subcellular compartments are known to have distinct pH, which is key for sustaining the biological processes inside them. For instance, the parasite cytosol maintains a static pH near 7.3[2], whereas the DV requires a lower pH near 5.0 for hemoglobin digestion[3-6]. The mitochondrion has a slightly basic pH (7.37 ± 0.09) whereas the apicoplast is more neutral (7.12 ± 0.40)[7].

Regulation of pH in distinct subcellular compartments involves multiple players, including buffers, enzymes, transporters, and proton pumps[8]. Proton pumps are critical because they can directly transport protons against the concentration gradient, actively regulating subcellular pH[9]. In *P. falciparum*, two types of proton pumps are present[10], including the pyrophosphate (PPi) driven H^+-pumping pyrophosphatases (H^+-PPases) or vacuolar pyrophosphatases (V-PPases)[11-13], and the ATP driven vacuolar type ATPases (V-type ATPases)[14]. VP1 (vacuolar pyrophosphatase 1) is an example of PPi driven proton pumping pyrophosphatase. In *P. falciparum*, a recent study has shown that VP1 is mainly localized on the parasite plasma membrane, regulates cytosolic pH, and plays essential roles in the ring stage and the ring-to-trophozoite transition[15]. On the other hand, V-type ATPase is a large molecular weight ATP hydrolyzing proton pumping machinery[16], consisting of a V_1 domain containing subunits of A-H and a V_o domain containing subunits of a, c, c', c'', d, e. The cytosolic V_1 domain holds the ATP hydrolysis hexamer made of A and B subunits, whereas the membrane bound V_o domain contains the H^+ channel, which is involved in proton transport across the membrane. A unique feature of this machinery lies in the reversible assembly and disassembly of the V_1V_o domains[17], regulating the pump's function in response to various extracellular conditions[18]. The *P. falciparum* genome encodes all V_1 domain subunits and most V_o domain subunits that are present in other eukaryotes (www.PlasmoDB.org). The recent genome-wide mutagenesis study in *P. falciparum*[19] and the knockout survey in *P. berghei*[20] reveal that nearly all V-type ATPase subunits are essential in the asexual blood stage. Despite the significance, our understanding of the physiological role of V-type ATPase in malaria parasites remains rather limited.

In classical model organisms, including yeast, humans, and plants, V-Type ATPase is localized on the membranes of multiple subcellular compartments such as endosome, lysosomes, vacuoles, Golgi, and the plasma membrane[21-23]. In marine phytoplankton such as diatoms, dinoflagellates and coccolithophores, V-type ATPase localizes to the membranes of chloroplasts derived from endosymbiosis and significantly enhances carbon fixation and oxygen production[24]. In *P. falciparum*, previous studies have suggested that V-type ATPase is a major proton pump responsible for maintaining cytosolic pH[2] and DV pH[5] in trophozoite-stage

parasites. However, its localization has remained elusive or somewhat controversial. An early study indicated that V-type ATPase has heterogenous but not well-defined localization[25]. In another study, immunofluorescence assays (IFAs) and immuno-EM suggested that V-type ATPase is localized on the parasite periphery, DV, and small clear vesicles[26]. However, the use of antibodies raised against the subunits of the bovine V-type ATPase in the study[26] was likely problematic due to limited specificity towards the *Plasmodium* counterparts. Furthermore, another report revealed that V-type ATPase also localizes on the RBC membrane, apparently being exported to the RBC cytosol[27]. Thus, studies of the *Plasmodium falciparum* V-type ATPase have not provided a consensus on its localization. Therefore, further investigation is needed to clarify the localization and function of this important proton pump in malaria parasites.

In this study, we employed genetic and biochemical approaches to better understand the localization and functionality of V-type ATPase in *P. falciparum*. Our data suggest that V-type ATPase is expressed throughout the IDC and exhibits dynamic localization patterns that vary depending on the specific developmental stages of the parasite. We have also discovered the intriguing localization of V-type ATPase on rhoptries and secretory vesicles in merozoites. Moreover, our results underscore the essentiality of V-type ATPase throughout the IDC. Depletion of the proton pump leads to the arrest of trophozoites, which contain undigested hemoglobin in the DV. Using the V-type ATPase specific inhibitor Bafilomycin A1, we have discovered that V-type ATPase potentially plays important roles during parasite egress and invasion. Finally, our study demonstrates that the V-type ATPase is sensitive to disruption by Bafilomycin A1, but the complex stability is less susceptible to certain treatments, such as low glucose or chloroquine.

Results

Endogenous tagging of V_1A via CRISPR/Cas9 for localization and conditional knockdown

The highly conserved V-Type ATPase has 2 domains, the V_1 domain that hydrolyses ATP and the V_o domain carrying out proton translocation using the free energy released from ATP hydrolysis. *P. falciparum* encodes all subunits required to form the V_1 subunit, including subunits of A (PF3D7_1311900), B (PF3D7_0406100), C (PF3D7_0106100), D (PF3D7_1341900), E (PF3D7_0934500), F (PF3D7_1140100), G (PF3D7_1323200), and H (PF3D7_1306600). The V_o includes subunits of a (PF3D7_0806800), c (PF3D7_0519200), c'' (PF3D7_1354400) and e (PF3D7_0721900). Subunits A and B form the ATP hydrolyzing hexamer to power the rotational movement of the entire proton pump. To study V-type ATPase in *P. falciparum*, we successfully tagged the endogenous locus of subunit A (V_1A) C-terminally with the triple HA epitope (3xHA) and elements required for conditional knockdown using the TetR-DOZI-aptamer system[28,29]. This was achieved via CRISPR/Cas9[30,31] with two different gRNA plasmids (**Figure 1A**). We termed the resulted transgenic parasite line NF54attB-V_1A-3HA^{apt}. We also performed limiting dilution to clone the transgenic parasite line to obtain pure parasites. The D11 clone was chosen for all subsequent experiments. The genotype of the NF54attB-V_1A-3HA^{apt} line (D11 clone) was verified by diagnostic PCR (**Figure 1B**). The expression of V_1A-3HA proteins at the expected molecular weight was confirmed by Western blot (**Figure 1C**).

To verify the localization of V-type ATPase in *P. falciparum*, we tightly synchronized the parasites with alanine/HEPES and performed Immunofluorescence studies (IFAs) over the 48 h lifecycle. We used Exp2[32], the maker for the Parasitophorous Vacuolar Membrane (PVM), as the indicator of the parasite periphery. From the time of invasion (T0), we harvested samples every 8 hours in

128 the ring stage and every 4 hours in trophozoite or schizont stages. V_1A was seen to be
129 expressed in all asexual blood stages (**Figure 2A**). In the ring stage, V_1A localized to the
130 parasite periphery, showing good colocalization with Exp2. In the trophozoite stage, V_1A was
131 predominantly localized on both the Parasite Plasma Membrane (PPM) and the Digestive
132 Vacuole (DV). This localization pattern was also observed in the early schizont stage. However,
133 in the late schizont stage, some punctate signals appeared near the parasite periphery. To
134 further characterize this, we performed IFA on schizonts pre-treated with the egress inhibitor,
135 ML10[33], a reversible blocker of protein kinase G. Treatment of ML10 inhibits parasite egress,
136 leading to an increased number of mature late schizont stage parasites. In the treated mature
137 schizonts, V_1A's localization appeared more punctate, lacking confined signals showing circular
138 or membranous structures (**Figure 2B**). This prompted us to further verify V-type ATPase's
139 localization via Immuno-Electron Microscopy. Indeed, immuno-EM revealed a specific
140 localization of V_1A on rhoptries and some small vesicles near them (**Figure 3**), indicating that V-
141 type ATPase is also present on the secretory organelles in merozoites. Altogether, we have
142 used IFA and Immuno-EM to uncover the dynamic localization of V-type ATPase in different
143 asexual stages of *P. falciparum*. This dynamic localization of V-type ATPase may be associated
144 with its multifunctionality throughout the 48 h lifecycle.

145 **V-type ATPase is essential for asexual growth and development in *P. falciparum***

146 To understand the essentiality of V-type ATPase in *P. falciparum*, we performed knockdown
147 studies using two different methods to remove aTc. In the first method, we synchronized the
148 parasites several times and started aTc removal in the early ring stage (**Figure 4A**). The
149 knockdown parasites appeared healthy 24 h post aTc removal, but they failed to produce any
150 new ring stage parasites in the next 24 h. At 48 h of knockdown, the parasites were arrested in
151 the trophozoite stage and lysed at 72 h. Thus, V_1A knockdown from the early ring stage resulted
152 in trophozoite arrestment and parasite demise within one cycle. In the second method, we
153 started aTc removal from the synchronized trophozoite stage parasites (**Figure 4D**). The
154 knockdown parasites were able to produce new ring stage parasites at 24 h post aTc removal,
155 but were arrested again in the trophozoite stage at 48 h. The arrested parasites did not initiate
156 another IDC, but remained arrested or lysed at 72 h. Thus, both knockdown methods revealed
157 the essentiality of V-type ATPase for asexual growth and development in *P. falciparum*. In each
158 experiment, quantification of parasite growth in the aTc (±) conditions was shown in **Figure 4B**
159 **and 4E**. The V_1A protein levels of the knockdown experiments were shown by Western blot in
160 **Figure 4C and 4F**.

161 To better understand parasite developmental blockage upon V_1A knockdown, we observed the
162 morphological changes of the parasites in a more detailed time course experiment (**Figure 4G**).
163 In tightly synchronized parasites, we collected thin blood smears every 8 hours during the ring
164 stage and every 4 hours during the trophozoite and schizont stages. Unlike the aTc (+) parasites
165 that completed their development normally, we observed an arrest in parasite growth in the aTc
166 (-) culture at 32 h post aTc removal. The knockdown parasites were arrested in the mid-
167 trophozoite stage and did not progress significantly in the remaining hours of the IDC.
168 Altogether, using different approaches, we have shown that knockdown of V-type ATPase leads
169 to the arrest of parasite development in the trophozoite stage within one IDC post aTc removal.
170 Overall, our results confirm that V-type ATPase is essential for *P. falciparum*, with the
171 trophozoite stage being the most susceptible to the loss of this proton pump.

172 **V-type ATPase is essential for hemoglobin digestion**

173 V-type ATPase has been shown to regulate the pH of DV in trophozoite stage parasites[3-5]. A low
174 pH (~ 5.0) is essential for hemoglobin digestion, which is extremely important for malaria
175 parasites to obtain nutrients and gain space to grow inside RBCs[34]. To get a deeper
176 understanding of the knockdown effects on the DV, we performed Transmission Electron
177 Microscopy (TEM) studies. The knockdown experiment was initiated from Percoll-enriched
178 schizont stage parasites, and we purified parasites by a magnetic column at 36 h post aTc
179 removal. The parasitemia of both aTc (±) cultures reached nearly 100% (**Figure 5A**). The aTc (-)
180 culture displayed more cell lysis compared to the aTc (+) culture after magnetic enrichment,
181 indicating that the integrity of some arrested trophozoites was compromised. Under TEM, the
182 knockdown parasites exhibited striking features (**Figure 5B**). The DV of knockdown parasites
183 showed significantly higher electron density than the control. Additionally, we observed
184 membrane-bound large vesicles inside the DV, indistinguishable from the RBC cytosol in terms
185 of electron density. These structures apparently contained large amounts of undigested
186 hemoglobin. Although not measured quantitatively, we also noticed a significant reduction in
187 hemozoin crystals in the knockdown parasites compared to the control. Consequently,
188 knockdown of V-type ATPase leads to defects in several steps of hemoglobin metabolism,
189 including the release of hemoglobin into the DV, breakdown of hemoglobin into small peptides,
190 and formation of hemozoin.

191 Hemoglobin uptake is initiated at a specialized structure called cytostome[35], and hemoglobin-
192 containing vesicles (HCvs) are pinched off from the membranes and fused with the DV to
193 release their contents for proper digestion and heme detoxification. The hemoglobin containing
194 vesicles are thus wrapped with two membranes, with the PPM on the outside and the PVM on
195 the inside[36]. Interestingly, knockdown of V-type ATPase blocked hemoglobin digestion in the DV,
196 but the upstream trafficking of HCvs enroute to the DV was seemingly not affected. This differed
197 from a previous study that showed accumulation of HCvs inside the parasite cytosol upon
198 conditional inactivation of PfVPS45[37], a protein involved in vesicular trafficking. Moreover, the
199 fusion of the outer membrane of HCVs to the DV membrane is potentially a rapid process as
200 this event has been rarely observed in wildtype parasites[38]. In the V_1A knockdown parasites, the
201 undigested hemoglobin was surrounded by a single membrane (**Figure 5B, red arrows**). This
202 information indicated that fusion of HCVs with the DV membrane was likely normal upon
203 depletion of V-type ATPase, but degradation of the inner membrane of HCvs was blocked.
204 Interestingly, we also observed that some vesicles in the DV of the knockdown parasites had
205 much reduced electron density, likely due to a more advanced level of hemoglobin digestion
206 (**Figure 5B, blue arrow**). Overall, our results show that V-type ATPase is critical for hemoglobin
207 release and digestion in the DV.

208 **V-type ATPase is essential for regulating cytosolic pH**

209 Apart from its role in the DV, V-type ATPase is known to regulate cytosolic pH by pumping
210 protons across the PPM in *P. falciparum*[2]. This understanding was based on the observation
211 that Bafilomycin A1, an inhibitor of V-type ATPase, caused a dramatic decline of cytosolic pH. A
212 recent study suggests that Bafilomycin A1 causes a stearic hinderance and blocks the c-ring
213 rotation by preventing the interaction between subunit a and the c-ring[39]. The effect of V-type
214 ATPase on cytosolic pH, however, has not been confirmed by genetic studies in *Plasmodium*. To
215 address this, we utilized the well-established pH measurement technique with BCECF-AM (2',7'-
216 Bis-(2-Carboxyethyl)-5-(and-6)-Carboxyfluorescein, Acetoxymethyl Ester) in saponin-treated
217 trophozoites[2]. We quantified cytosolic pH of aTc ± cultures at 36 h post knockdown from Percoll-

218 enriched schizont stage parasites. We included Bafilomycin A1 as a positive control. Our assays
219 revealed that cytosolic pH was 7.24±0.08 in the control parasites but reduced to 6.01±0.28 upon
220 knockdown of V-type ATPase (**Figure 6**). This result confirms that V-type ATPase is the major
221 proton pump for regulating cytosolic pH in trophozoite stage parasites. Consistent with the
222 published data[2], we also observed that Bafilomycin A1 caused a profound decrease in cytosolic
223 pH from 7.24 to 6.51±0.1 within 5 min of treatment. Interestingly, the combination of V_1A
224 knockdown and Bafilomycin A1 resulted in an even lower cytosolic pH (5.77±0.15), although this
225 effect was not statistically significant compared to knockdown alone ($p > 0.05$). Overall, our
226 findings confirm that V-type ATPase plays a major role in regulating cytosolic pH in the
227 trophozoite stage parasites.

228 **Viability of the V-type ATPase knockdown parasites**

229 Our data have shown that knockdown of V-type ATPase led to the arrest of trophozoite-like
230 parasites that contained large amounts of undigested hemoglobin in the DV and reduced
231 cytosolic pH. To understand the viability of these parasites, we performed an aTc addback
232 experiment post knockdown (**Figure 7A**). We initiated the knockdown from tightly synchronized
233 Percoll-enriched schizont stage parasites, and performed the addback at different time points
234 post knockdown, 28 h, 36 h, 40 h, and 48 h. Consistent with **Figure 4G**, the knockdown
235 parasites at 28 h did not display obvious morphological defects in Giemsa-stained smears
236 (**Figure 7B**). Upon aTc addback, these parasites were able to produce new ring stage parasites
237 in the next 24 h. At 36 h post knockdown, a delay in parasite development was readily
238 detectable. Upon addback, however, most of the arrested parasites managed to produce new
239 ring stage parasites in the next 24 h. These ring stage parasites continued to become
240 trophozoites at 48 h of addback. This result suggested that the arrested parasites at 36 h post
241 knockdown remained largely viable, despite having severe defects in hemoglobin digestion and
242 pH regulation. At 40 h post knockdown, a smaller percentage of the arrested parasites still
243 succeeded in producing new ring stage parasites at 24 h post addback. However, just a few
244 hours later at 48 h post knockdown, aTc addback failed to rescue any parasite growth. The
245 knockdown parasites either displayed abnormal morphologies or lysed. Altogether, these results
246 imply that *P. falciparum* parasites can sustain viability in a severely stressed condition for at
247 least several hours. Remarkably, aTc addback allowed the arrested parasites to recover from
248 various defects caused by V_1A knockdown, such as reduced cytosolic pH, blockage of
249 hemoglobin digestion in the DV, and other possible disruptions.

250 **The effect of Bafilomycin A1 on parasite egress and invasion**

251 The localization of V-type ATPase on rhoptries and other secretory organelles prompted us to
252 investigate the potential role of this proton pump in parasite egress and invasion. However, in
253 our knockdown studies initiated from the ring, trophozoite, or schizont stage (**Figures 4-7**), an
254 extended period of ~ 30 h was consistently required before the onset of detectable defects. In
255 addition, all knockdown approaches led to the arrest of trophozoites, making examinations of
256 schizonts infeasible. To address the delayed effects of genetic knockdown, we reasoned that a
257 pool of pre-existing V_1A proteins, present before aTc removal, might permit parasite survival and
258 maturation over an extended period until the proteins were fully exhausted. To overcome this
259 limitation, we used Bafilomycin A1 to rapidly block V-type ATPase in the late schizonts and
260 observed its effect on parasite egress and invasion. As shown previously, Bafilomycin A1
261 reduced cytosolic pH from ~ 7.3 to ~ 6.5 in about 5 min in *in vitro* assays (**Figure 6**).

262 In brief, we tightly synchronized the parasites with alanine/HEPES and used ML10 to block
263 parasite egress, thereby increasing the percentage of mature schizonts. At the mature schizont
264 stage (~ 0 h), we added Bafilomycin A1 (100 nM) for 2 h, washed it out, and allowed parasites
265 to invade new RBCs for 4 h. At 6 h post the initiation of the experiment, we counted the
266 parasitemia of newly formed ring stage parasites and used it as the readout of successful
267 egress and invasion (**Figure 8A**). Parasite growth and morphology were also examined at 24 h
268 and 48 h post the initiation of the experiment. At 6 h, while the new ring stage reached
269 4.77%±0.25% in the control culture, the Bafilomycin A1 treated culture had a significantly lower
270 parasitemia (0.24%±0.07%) (**Figure 8B**). In the treated culture, events of merozoite invasion
271 were commonly observed, however, formation of new rings was drastically reduced (**Figure**
272 **8C**). In the next 24 h and 48 h, the control culture followed the normal progression of the
273 lifecycle. In contrast, the treated culture barely increased parasitemia (**Figure 8B**). The
274 parasites displayed abnormal morphologies or failed to invade RBCs. It was interesting to note
275 that in the treated culture, some merozoite-like parasites appeared to be attached to the RBC
276 surface even at 48 h post the initiation of the experiment (**Figure 8C**). Collectively, treatment of
277 Bafilomycin A1 in the mature schizont stage leads to dramatic reduction in the formation of new
278 ring stage parasites.

279 **Stability of the V-type ATPase complex under various conditions**

280 In model eukaryotes, it has been well established that V-type ATPase undergoes a reversible
281 process of assembly and disassembly to rapidly regulate its function upon encountering
282 different conditions[17]. For example, the yeast V-type ATPase is very sensitive to the bioenergetic
283 status of the cell and V_1 and V_o disassociate in a low glucose condition[40]. Disassociation of the
284 two domains completely abolishes the proton pumping function as well as the ATP hydrolysis
285 activity of the V_1 domain[41]. To assess if the *Plasmodium falciparum* V-type ATPase can regulate
286 its function by changing complex stability, we treated synchronized trophozoite stage parasites
287 with Bafilomycin A1, chloroquine, and 1 mM glucose and verified V_1V_o complex formation
288 through BN/PAGE. In parallel, the expression level of the V_1A monomers was monitored by
289 SDS/PAGE. As shown in **Figure 9**, in the control protein lysate, we detected a high-molecular-
290 weight band near the marker of 1.026 MDa, which approximately corresponded to the total
291 molecular weights of the entire V-type ATPase[21]. In addition, in BN/PAGE, smaller bands near
292 the markers of 720 kDa, 240 kDa, and 66 kDa were also detected. The nature of these smaller
293 complexes is uncertain at present. They could be assembly intermediates of the V_1V_o complex
294 or electrophoretic degradation products, although enough protease inhibitor cocktails were
295 included throughout the experiment. Upon Bafilomycin A1 (10 nM) treatment, the top band near
296 1.026 MDa was detectable after 2 h, but gradually decreased in intensity after 4 h and 8 h. By
297 contrast, the monomer V_1A remained more stable throughout the time course. This result
298 indicated that the V-type ATPase dissembled upon Bafilomycin A1 treatment longer than 2 h.
299 Upon treatment with chloroquine (100 nM) or 1 mM glucose, however, the top band near 1.026
300 MDa remained largely constant even after 8 h. The V_1A monomer was stably expressed in
301 chloroquine treated samples and gradually decreased in the low glucose treated samples.
302 Together, these data implied that the V-type ATPase complex was readily disrupted by
303 Bafilomycin A1, but not by treatment of chloroquine or a low glucose condition.

304 **Discussion**

305 In this study, we have characterized the essentiality, localization, and biological function of V-
306 type ATPase in *Plasmodium falciparum*. By tagging the subunit A of V_1 via CRISPR/Cas9, we

307 generated a conditional knockdown parasite line under aTc regulation and obtained several
308 interesting results.

309 We have found that V-type ATPase is essential for *P. falciparum* during asexual growth and
310 development, with the trophozoite stage being particularly vulnerable to death when this proton
311 pump is depleted (**Figures 4-7**). The localization of *P. falciparum* V-type ATPase is highly
312 dynamic throughout the 48 h asexual lifecycle (**Figures 2-3**). Specifically, in trophozoite stage
313 parasites, V-type ATPase localizes on both the parasite plasma membrane (PPM) and digestive
314 vacuole (DV). This localization pattern is consistent with its role in regulating cytosolic pH[2] and
315 DV pH[5]. We also observed a drastic reduction in cytosolic pH in the V_1A knockdown parasites
316 during the trophozoite stage (**Figure 6**). Moreover, our data suggest that V-type ATPase is also
317 expressed and localized on the PPM in the ring stage. However, we need to be cautious when
318 defining the precise localization of V-type ATPase in the small ring stage parasites. A recent
319 study implied that V-type ATPase might not play a major role in proton pumping during the ring
320 stage, as the pyrophosphate driven proton pump, PfVP1, is essential for this stage[15].
321 Conditional depletion of PfVP1 blocks ring stage development and the ring-to-trophozoite
322 transition, which is apparently not rescued by the V-type ATPase. This indicates that V-type
323 ATPase might either not fulfill proton pumping across the PPM in the ring stage or have a
324 negligible role. In the late schizont stage, we have observed punctate signals of V_1A in IFA
325 without defined membranous staining (**Figure 2B**). Immuno-EM further revealed V_1A's
326 localization on rhoptries and secretory organelles near rhoptries (**Figure 3**). To our best
327 knowledge, this is the first report that observed such localization of V-type ATPase on mature
328 secretory organelles in protozoa. A previous study highlighted the function of V-type ATPase in
329 facilitating the maturation of secretory organelles in *Toxoplasma gondii*, an apicomplexan
330 parasite related to *Plasmodium*[42], but the presence of V-type ATPase on mature rhoptries or
331 micronemes was not detected[42]. Thus, the unique localization of V-type ATPase on rhoptries
332 and secretory organelles in *Plasmodium* has led us to investigate the role of this proton pump in
333 parasite egress and invasion. To alleviate the slow effect of genetic knockdown, we used
334 Bafilomycin A1 to chemically inhibit V-type ATPase in a short time (2 h) and observed serious
335 defects of the parasites in initiating the next lifecycle (**Figure 8**). Bafilomycin A1's specificity as a
336 V-type ATPase blocker has been well documented and it has been used as a standard reagent
337 in *P. falciparum* studies[2,5]. We quantified the number of new ring stage parasites post
338 Bafilomycin A1 treatment and used it as a readout to indicate the overall effects on parasite
339 egress and invasion. However, our data did not provide detailed mechanisms underlying the
340 mode of action of Bafilomycin A1 in mature schizont stage parasites. It is possible that
341 Bafilomycin A1 exerts its effects through multiple mechanisms, such as killing the schizonts,
342 blocking egress, and inhibiting invasion. Future investigations will be necessary to characterize
343 these processes in detail. Nevertheless, our data implied that V-type ATPase likely plays a role
344 in parasite egress and invasion.

345 In the trophozoite stage, we have discovered that V-type ATPase is extremely important for
346 hemoglobin digestion in the DV. This finding aligns with the previously reported role of V-type
347 ATPase in maintaining DV pH[5]. However, observation of undigested hemoglobin in the DV of
348 V_1A knockdown parasites was astonishing and stands out as a novel finding of this study
349 (**Figure 5**). To date, the processes of hemoglobin uptake from cytostomes and the delivery of
350 hemoglobin containing vesicles (HCvs) to the DV remain enigmatic in *P. falciparum,* as these
351 processes are likely dynamic, transient, and difficult to capture. A previous study reported the
352 rare fusion of one HCv with the DV membrane among > 600 examined thin sections under

353 transmission electron microscopy[38]. Since cytostomes are invaginated from the PPM and PVM,
354 the HCvs are enclosed by the PPM on the outside and the PVM on the inside. The fusion event
355 indicates that the PPM of HCvs fuses with the DV membrane[38]. Therefore, the membrane
356 surrounding the undigested hemoglobin in our data should be the PVM, not the PPM. We can
357 speculate that after HCvs are fused with the DV membrane, the leftover PVM needs to be
358 digested first by specific enzymes (likely lipases) before hemoglobin can be digested by aspartic
359 proteases and cysteine proteases[43]. The enzyme responsible for digesting the PVM of HCvs
360 remains unknown, but it is evidently pH dependent and not among the list of enzymes known to
361 digest hemoglobin[44].

362 Moreover, we have detected the native *P. falciparum* V-type ATPase complex by BN/PAGE. In
363 addition to the large molecular weight band near 1.0 MDa, many smaller subcomplex-like
364 moieties were also detected at various molecular weights (**Figure 9**). Though unknown, we
365 speculate that formation of the *P. falciparum* V-type ATPase complex is a highly regulated
366 process, and the intermediate complexes might be involved in the assembly and/or disassembly
367 processes. In mammalian cells, the V-type ATPase was also examined by BN/PAGE but few
368 intermediate complexes were detected[45]. In addition, we noted that the complex was readily
369 disrupted upon Bafilomycin A1 treatment but remained more stable upon challenges of
370 chloroquine and low glucose. The glucose effect on *P. falciparum* V-type ATPase was not
371 expected since low glucose levels are known to dissociate the complex in yeast[40]. This could
372 reflect the unique features of V-type ATPase in *P. falciparum* in a bioenergetically different
373 environment from that of yeast.

374 In summary, our data have provided valuable insights into the localization and functions of V-
375 type ATPase in *Plasmodium falciparum*, highlighting its critical roles in regulating pH in various
376 subcellular compartments. As we prepared this manuscript, a very recent report by Alder and
377 colleagues also unveiled the localization and function of the *P. falciparum* V-type ATPase, using
378 an inducible knockout approach[46]. Their study has characterized defects related to knockdown
379 of subunit B in the V_1 domain and subunits a and c in the V_o domain. Interestingly, our findings
380 from knockdown of V_1A align well with those obtained from inducible knockout of V_1B. Given
381 that subunits A and B work together in the ATP hydrolysis center, genetic knockdown (or
382 knockout) of either A or B leads to common downstream effects. Nonetheless, the combined
383 studies on the two major subunits of V-type ATPase, both from our work and others[46], have
384 collectively revealed the dynamic localization of V-type ATPase in the asexual blood stage of *P.*
385 *falciparum*. These studies shed light on the significant role of V-type ATPase in parasite growth
386 and replication, thereby enhancing our understanding of *Plasmodium* biology. Moreover, results
387 of our work and Alder *et al.*[46] could provide valuable guidance for drug development strategies
388 as V-type ATPase was implicated as a drug target[47,48].

389

390 **Figure Legends**

391 **Figure 1. Endogenous tagging of V_1A via CRISPR/Cas9 for conditional expression**

392 **A**, Schematic of modifying the V_1A genetic locus via CRISPR/Cas9 mediated double crossover
393 recombination. The primer positions were indicated by black arrows with sequences listed in
394 Table 1.
395

396 **B**, Diagnostic PCR/DNA electrophoresis showing the corrected modification of the V_1A genetic
397 locus in the D11 clone of NF54attB-V_1A-3HA^{apt}. The band sizes of PCR products were 0.8 kb
398 (lane 1), 1.2 kb (lane 4), and 1.9 kb (lane 8). One non-specific band was detected in lane 1
399 (star).
400
401 **C**, Western blot showing the expression of V_1A-3HA proteins in the transgenic parasite line,
402 NF54attB-V_1A-3HA^{apt}.
403
404 **Figure 2. Localization of V_1A throughout the asexual blood stages**

405 **A**, Localization of V_1A throughout the lifecycle. In the NF54attB-V_1A-3HA^{apt} line, V_1A was
406 detected by anti HA and FITC-labeled secondary antibodies. Exp2 was detected by anti-Exp2[49]
407 and TRITC-labeled secondary antibodies.

408 **B**, Localization of V_1A in mature schizont stage parasites treated with ML10. The synchronized
409 late-trophozoite stage parasites were treated with 25 nM of ML10 for 14 h to reach the mature
410 schizont stage. V_1A was detected by anti HA and FITC-labeled secondary antibodies. DNA was
411 stained with DAPI.

412 In each condition, representative images of at least 25 parasites were shown.

413 **Figure 3. Localization of V_1A on secretory organelles in mature schizont stage parasites**

414 **A-F**, Detection of V_1A signals on rhoptries and secretory organelles near rhoptries in the
415 parasite line NF54attB-V_1A-3HA^{apt} by immuno-electron microscopy. Bars, 500 nm.

416 **G-H**, Negative control images with the primary antibody omitted throughout the experiment.
417 Bars, 500 nm.

418 **Figure 4. Essentiality of V-type ATPase in the asexual blood stages**

419 Giemsa-stained images showing parasite morphologies resulted from knocking down of V_1A
420 from the ring stage (**A**), or from the trophozoite stage (**D**), in the NF54attB-V_1A-3HA^{apt} line.

421 Quantification of parasitemia in the aTc +/- cultures (**B, E**). At each time point, parasitemia was
422 determined from counting 1000 RBCs under a light microscope. Error bars indicated the s.d. of
423 three technical measurements.

424 Western blot showing the expression level of V_1A in the knockdown experiments (**C, F**). The
425 same blot was re-probed with anti-Exp2 to show loading controls.

426 **G**, Giemsa-stained images showing parasite morphological changes over the time course
427 experiment.

428 Experiments of A-F were repeated three times. Panel G was repeated two times.

429 **Figure 5. V-type ATPase is essential for hemoglobin digestion in the digestive vacuole**

430 **A**, Giemsa-stained images of control and V_1A knockdown parasites enriched by a magnetic
431 column.

432 **B**, Electron Transmission Microscopic images of control and V_1A knockdown parasites. In the
433 aTc - parasites, many vesicles inside the digestive vacuole had electron dense signals and were

434 surrounded by membranes (red arrows). Some vesicles had translucent appearance but were
435 still surrounded by membranes (blue arrow).

436 **Figure 6. V-type ATPase regulates cytosolic pH in trophozoite stage parasites**

437 At 36 h post knockdown, aTc +/- cultures of the NF54attB-V_1A-3HA^{apt} line were subjected to pH
438 measurement using the BCECF-AM method in the absence of presence of 100 nM Bafilomycin
439 A1 (100 nM) for 5 min. Error bars indicated the s.d. of 3-4 measurements in each condition.
440 Statistical analysis was done by student t-test. This experiment was repeated two times.

441 **Figure 7. Viability of the V-type ATPase knockdown parasites**

442 **A**, Schematic diagram of the knockdown/addback experiment. At various time points post
443 knockdown, the cultures were fed with aTc + medium and further monitored for 48 h.

444 **B**, Giemsa-stained images showing morphological changes of the parasites upon aTc addback.

445 This experiment was repeated three times.

446 **Figure 8. Effects of Bafilomycin A1 on parasite egress and invasion**

447 **A**, Schematic illustration of the experimental design generated by BioRender. Mature schizont
448 stage parasites (NF54attB-V_1A-3HA^{apt} under 250 nM) were treated with Bafilomycin A1 (100
449 nM) for 2 h. The drug was washed out and parasites were allowed to invade new RBCs for 4 h.
450 At 6 h, the parasitemia of newly formed ring stage parasites was monitored. Parasite
451 morphology and number were further examined at 24 h and 4 h post the initiation of the
452 experiment. aTc (250nM) was maintained throughout the experiment.

453 **B**, Giemsa-stained imaging showing parasite morphologies in the control and treated cultures.

454 **C**, Quantification of parasite growth throughout the experiment. Parasitemia was determined by
455 counting 1000 RBCs in each smear under a light microscope. Error bars indicated the s.d. of 3
456 measurements at each time point.

457 This experiment was repeated five times.

458 **Figure 9. The stability of V-type ATPase complex under various conditions**

459 Synchronized trophozoite stage parasites (NF54attB-V_1A-3HA^{apt} under 250 nM) were treated
460 with Bafilomycin A1 (10 nM), Chloroquine (100 nM), or 1 mM glucose for 2 h, 4 h, and 8 h.
461 Samples were harvested and analyzed by BN-PAGE and SDS-PAGE. The arrow indicated the
462 large molecular weight band corresponding to the estimated size of the *P. falciparum* V-type
463 ATPase. aTc (250nM) was maintained throughout the experiment.

464

465

466

467

468

469

470 **Materials and Methods**

471 **Table 1. Primers and oligoes used in this study**

ID	PRIMER NAME	SEQUENCE
P1	A-VATPase gRNA1	TCATATTAAGTATATAATATTAGTAGGTTTAAGAAACTTGAGTTTCAGAGCTATGCTGGA
P2	A-VATPase gRNA2	CATATTAAGTATATAATATTGAAACTTGATGGAAAAATGATGTTTCAGAGCTATGCTGGA
P3	A-VATPase gRNA1-N20	AGTAGGTTTAAGAAACTTGA
P4	A-VATPase gRNA2-N21	GAAACTTGATGGAAAAATGAT
P5	N20CheckR	ATATGAATTACAAATATTGCATAAAGA
P6	RevOligo	TAGGAAATAATAAAAAAGCACCGACTCG
P7	Super CPF1	CTTTTATTTTTACTGTAATATAATTTTTTATAATGTAAAAATAAAGGG
P8	A-VATPase 5HRF	gatatctacgatatcccgcggtccggaGGTTCTCCATCTCGTATAGG
P9	A-VATPase 5HRR	ATGGTAACCTGcTTcTCCATaAgaTTaCgaAgtCCaACaGTTATTTCTTCTTCAAGTGCC
P10	A-VATPase 3UTRF	atgcgcgcGTGATTTATTTATTAGTTGAATAATTAAAGC
P11	A-VATPase 3UTRR	tccggaccgcgggatatcgtagatatcGAAAAAGTTTACCTTAGTATGATAAAAAAATG
P12	pMG75-BBHA REV	TGGGCCCGAATTCTCATCATTGTGC
P13	pMG75SeqF	CTTTAAATTCATGCAAAAATTTAC
P14	A-VATPase 5chk	GGTTATCCAGCTTATTTAGGTGC
P15	A-VATPase 3chk New	GATCTACTTACAATTTTTTTCCTTC

472

473

474 1, Plasmid Construction

475 Subunit A of *Plasmodium falciparum* V-Type ATPase (V_1A, PF3D7_1311900) was endogenously
476 tagged with a 3xHA epitope and the TetR-DOZI-Aptamer system at the C-terminus via
477 CRISPR/Cas9. Two NFCas9/gRNA constructs were made according to our cloning procedures
478 published earlier[50]. The DNA oligoes used for cloning and sequencing were listed in **Table 1**
479 (P1-P7). To make the pMG75 template plasmid for double crossover recombination, the 5' and
480 3' homologous regions (5'HR and 3'HR) of V_1A were PCR amplified from the wildtype genomic
481 DNA using primers P8 and P9 for 5'HR and P10 and P11 for 3'HR. The PCR product was
482 purified and then digested with SacII/BstEII for 5'HR and BssHII/SacII for 3'HR. The digested
483 fragments were sequentially cloned into the pMG75 vector bearing Blasticidin deaminase by T4
484 DNA ligase. The clones were screened by proper restriction digestion. The positive clones were
485 further confirmed by Sanger sequencing using the primers P12-P13. The final maxi-prep

plasmid of pMG75-BSD-V_1A-3HA was linearized with EcoRV before being transfected into parasites.

2, Parasite Culture and Transfection

Plasmodium falciparum wildtype strain NF54attB was generously provided by Dr. Joshua Beck (Iowa State University). This line is compatible with all three transfection markers that are commonly used, including BSD (Blasticidin deaminase), hDHFR (human dihydrofolate reductase) and yDHODH (yeast dihydroorotate dehydrogenase). *P. falciparum* was cultured in human O^+ red blood cells (5% hematocrit, Interstate Blood Bank, Inc.) in the standard RPMI 1640 medium containing 0.5% AlbuMAX® II (Invitrogen), 15 mM HEPES, 10 mg/L hypoxanthine, 25 mM $NaHCO_3$, and 50 mg/L gentamicin. Transfections were performed using the standard methods in the ring stage with details shown previously[50,51]. The concentration of aTc was 250 nM in all aTc (+) cultures.

3, Immunofluorescence assays (IFA)

Parasites were tightly synchronized with alanine (0.5 M)/HEPES (10 mM) several times. At each time point of the experiment, ~ 50 µL parasitized RBCs were collected and fixed with 4% paraformaldehyde, 0.0075% glutaraldehyde in 1X PBS. Blocking was done by 3% BSA/PBS for overnight at 4°C. Fixed cells were permeabilized by Triton X-100 (0.25%)/PBS and incubated with primary antibodies overnight at 4°C, including α-HA (1:300, mouse, sc-7392, Santa Cruz Biotechnology) and α-Exp2 (1:500, rabbit)[49]. Following thorough washing, the samples were incubated with FITC- or TRITC- labeled secondary antibodies for 3 h at room temperature. Other procedures followed standard IFA protocols. Images were captured using the Nikon Ti microscope.

4, Western Blot for BN-PAGE and SDS-PAGE

Parasite cultures were lysed by Saponin (0.05%)/PBS and host hemoglobin was removed by several washes with 1X PBS. From one culture condition, two aliquots of samples were obtained for BN-PAGE and SDS-PAGE, respectively. For BN-PAGE, the saponin lysed pellet was solubilized with 1% glycodiosgenin (GDN) in MESH buffer (250 mM sucrose, 10 mM HEPES, 1 mM EDTA, 1X protease inhibitor cocktail) for overnight at 4°C. The supernatant after a high-speed centrifugation (13,000 rpm, 10 min) was used for Blue-Native gel electrophoresis and Western blot. For SDS-PAGE, the saponin lysed pellet was solubilized by 2% SDS/Tris (65 mM, pH 6.8) for overnight at 4°C. The supernatant after a high-speed centrifugation (13,000 rpm, 10 min) was used for denatured electrophoresis. For all samples, the protein concentrations were determined by the Pierce™ BCA Protein Assay Kit (ThermoFisher Scientific) to ensure equal loading. Antibodies used for Western blot included α-HA (1:10,000, mouse, sc-7392, Santa Cruz Biotechnology), α-Exp2 (1:10,000, rabbit)[49], HRP-conjugated goat anti-mouse secondary (1:10,000, A16078, ThermoFisher Scientific), HRP-conjugated goat anti-rabbit secondary (1:10,000, 31460, ThermoFisher Scientific). The membranes were incubated with Pierce ECL Western Blot Substrates and developed using the Bio-Rad chemidoc imaging system.

5, Transmission Electron Microscopy

Parasites were synchronized with alanine (0.5 M)/HEPES (10 mM) several times and the schizont stage parasites were enriched by Percoll. After several washes with 1X PBS, the

528 schizonts were added with new RBCs and cultured in aTc +/- conditions for 36 h. Both cultures
529 were then passed through a MACS magnetic column (MiltenyiBiotec) to enrich trophozoite
530 stage parasites, which were fixed with freshly made 2% paraformaldehyde, 2.5% glutaraldehyde
531 in 100mM sodium cacodylate buffer for overnight at 4°C. The samples were shipped to Dr.
532 Wandy Beatty from the Molecular Microbiology Imaging Facility at Washington University, St.
533 Louis, MO for further processing and imaging. Other procedures were carried out as shown
534 previously[51].

535 6, Immuno-Electron Microscopy

536 Parasites were synchronized with alanine (0.5 M)/HEPES (10 mM) several times and the
537 trophozoite stage parasites were enriched using a MACS magnetic column (MiltenyiBiotec). The
538 enriched parasites were treated with 25 nM ML10[33] for 14 h and then fixed with freshly made
539 4% paraformaldehyde/0.05% glutaraldehyde/100mM PIPES buffer for overnight at 4°C. The
540 samples were shipped to Dr. Wandy Beatty from the Molecular Microbiology Imaging Facility at
541 Washington University, St. Louis, MO for further processing and imaging. Other procedures
542 were carried out as previously published[50]. Antibodies used in the study included α-HA (1:300,
543 mouse, sc-7392, Santa Cruz Biotechnology) and goat anti-mouse IgG 18 nm colloidal gold-
544 conjugated secondary antibody (1:100, Jackson ImmunoResearch Laboratories). A parallel
545 sample with the primary antibody omitted was used as the negative control, which did not react
546 to the secondary antibody.

547 7, pH measurement with BCECF-AM, a ratio-metric pH indicator

548 pH measurement was carried out according to the published protocols[2]. Post 36 h of aTc
549 removal, the control and knockdown cultures were incubated with 4 μM BCECF-AM (2',7'-Bis-
550 (2-Carboxyethyl)-5-(and-6)-Carboxyfluorescein, Acetoxymethyl Ester, Fisher Scientific) for 30
551 min at 37°C. Pluronic at 1:1000 dilution was added to increase cellular permeability to BCECF-
552 AM. The parasites were treated with rapid saponin lysis to remove hemoglobin. The pellet was
553 washed two times with saline/glucose buffer (NaCl 125 mM, KCl 5 mM, MgCl2 1 mM, glucose
554 20 mM, HEPES 25 mM, pH 7.4) and resuspended in 1 mL of warm saline/glucose buffer. The
555 sample's fluorescence was monitored using a fluorescence spectrometer (Hitachi F-7000) at
556 535 nm with excitation wavelengths set at 490/440 nm. When Bafilomycin A1 (100 nM) was
557 used in aTc +/- conditions, the drug was incubated with saponin-lysed and washed parasites for
558 5 min before they were further analyzed by Hitachi F-7000. The fluorescence ratios were back
559 calculated to pH values according to a linear regression curve generated from several known
560 pH standards (pH 6.8, 7.1, 7.4), as shown previously[2].

561 **Acknowledgement**

562 We are grateful for the technical assistance and intellectual input from members of the Center
563 for Parasitology at Drexel University College of Medicine. We thank Dr. Joshua Beck (Iowa
564 State University) for providing the parasite line, Drs. Jaquin Niles (MIT) and Sean Prigge (Johns
565 Hopkins University) for providing the TetR-DOZI-aptamer plasmids, Drs. Baker and Ooij for
566 providing the compound, ML10. We thank Dr. Wandy Beatty at Washington University in St.
567 Louis for performing transmission electron microscopy and immuno-electron microscopy
568 studies.

569

570 **References**

571 1 WHO. World Malaria Report. (2022).
572 2 Saliba, K. J. & Kirk, K. pH regulation in the intracellular malaria parasite, Plasmodium
573 falciparum. H(+) extrusion via a V-type H(+)-ATPase. *J Biol Chem* **274**, 33213-33219
574 (1999). https://doi.org:10.1074/jbc.274.47.33213
575 3 Kuhn, Y., Rohrbach, P. & Lanzer, M. Quantitative pH measurements in Plasmodium
576 falciparum-infected erythrocytes using pHluorin. *Cell Microbiol* **9**, 1004-1013 (2007).
577 https://doi.org:10.1111/j.1462-5822.2006.00847.x
578 4 Bennett, T. N. *et al.* Drug resistance-associated pfCRT mutations confer decreased
579 Plasmodium falciparum digestive vacuolar pH. *Mol Biochem Parasitol* **133**, 99-114
580 (2004). https://doi.org:10.1016/j.molbiopara.2003.09.008
581 5 Saliba, K. J. *et al.* Acidification of the malaria parasite's digestive vacuole by a H+-
582 ATPase and a H+-pyrophosphatase. *J Biol Chem* **278**, 5605-5612 (2003).
583 https://doi.org:10.1074/jbc.M208648200
584 6 Klonis, N. *et al.* Evaluation of pH during cytostomal endocytosis and vacuolar catabolism
585 of haemoglobin in Plasmodium falciparum. *Biochem J* **407**, 343-354 (2007).
586 https://doi.org:10.1042/BJ20070934
587 7 Mohring, F. *et al.* Determination of glutathione redox potential and pH value in
588 subcellular compartments of malaria parasites. *Free Radic Biol Med* **104**, 104-117
589 (2017). https://doi.org:10.1016/j.freeradbiomed.2017.01.001
590 8 Casey, J. R., Grinstein, S. & Orlowski, J. Sensors and regulators of intracellular pH. *Nat*
591 *Rev Mol Cell Biol* **11**, 50-61 (2010). https://doi.org:10.1038/nrm2820
592 9 Cosse, M. & Seidel, T. Plant Proton Pumps and Cytosolic pH-Homeostasis. *Front Plant*
593 *Sci* **12**, 672873 (2021). https://doi.org:10.3389/fpls.2021.672873
594 10 Ginsburg, H. Abundant proton pumping in Plasmodium falciparum, but why? *Trends*
595 *Parasitol* **18**, 483-486 (2002). https://doi.org:10.1016/s1471-4922(02)02350-4
596 11 McIntosh, M. T. & Vaidya, A. B. Vacuolar type H+ pumping pyrophosphatases of parasitic
597 protozoa. *Int J Parasitol* **32**, 1-14 (2002). https://doi.org:10.1016/s0020-7519(01)00325-3
598 12 McIntosh, M. T., Drozdowicz, Y. M., Laroiya, K., Rea, P. A. & Vaidya, A. B. Two classes of
599 plant-like vacuolar-type H(+)-pyrophosphatases in malaria parasites. *Mol Biochem*
600 *Parasitol* **114**, 183-195 (2001). https://doi.org:10.1016/s0166-6851(01)00251-1
601 13 Luo, S., Marchesini, N., Moreno, S. N. & Docampo, R. A plant-like vacuolar H(+)-
602 pyrophosphatase in Plasmodium falciparum. *FEBS Lett* **460**, 217-220 (1999).
603 https://doi.org:10.1016/s0014-5793(99)01353-8
604 14 Karcz, S. R., Herrmann, V. R. & Cowman, A. F. Cloning and characterization of a
605 vacuolar ATPase A subunit homologue from Plasmodium falciparum. *Mol Biochem*
606 *Parasitol* **58**, 333-344 (1993). https://doi.org:10.1016/0166-6851(93)90056-4
607 15 Omobukola Solebo, L. L., Jing Zhou, Tian-min Fu, Hangjun Ke. Malaria parasites utilize
608 pyrophosphate to fuel an essential proton pump in the ring stage and the transition to
609 trophozoite stage. *BioRxiv* (2021). https://doi.org:doi:
610 https://doi.org/10.1101/2021.10.25.465524
611 16 Vasanthakumar, T. & Rubinstein, J. L. Structure and Roles of V-type ATPases. *Trends*
612 *Biochem Sci* **45**, 295-307 (2020). https://doi.org:10.1016/j.tibs.2019.12.007
613 17 Kane, P. M. Disassembly and reassembly of the yeast vacuolar H(+)-ATPase in vivo. *J*
614 *Biol Chem* **270**, 17025-17032 (1995).
615 18 Wang, H. & Rubinstein, J. L. CryoEM of V-ATPases: Assembly, disassembly, and
616 inhibition. *Curr Opin Struct Biol* **80**, 102592 (2023).
617 https://doi.org:10.1016/j.sbi.2023.102592

618 19 Zhang, M. *et al.* Uncovering the essential genes of the human malaria parasite
619 Plasmodium falciparum by saturation mutagenesis. *Science* **360** (2018).
620 https://doi.org:10.1126/science.aap7847
621 20 Bushell, E. *et al.* Functional Profiling of a Plasmodium Genome Reveals an Abundance
622 of Essential Genes. *Cell* **170**, 260-272 e268 (2017).
623 https://doi.org:10.1016/j.cell.2017.06.030
624 21 Harrison, M. A. & Muench, S. P. The Vacuolar ATPase - A Nano-scale Motor That Drives
625 Cell Biology. *Subcell Biochem* **87**, 409-459 (2018). https://doi.org:10.1007/978-981-10-
626 7757-9_14
627 22 Graham, L. A., Flannery, A. R. & Stevens, T. H. Structure and assembly of the yeast V-
628 ATPase. *J Bioenerg Biomembr* **35**, 301-312 (2003).
629 https://doi.org:10.1023/a:1025772730586
630 23 Lupanga, U. *et al.* The Arabidopsis V-ATPase is localized to the TGN/EE via a seed
631 plant-specific motif. *Elife* **9** (2020). https://doi.org:10.7554/eLife.60568
632 24 Yee, D. P. *et al.* The V-type ATPase enhances photosynthesis in marine phytoplankton
633 and further links phagocytosis to symbiogenesis. *Curr Biol* **33**, 2541-2547 e2545 (2023).
634 https://doi.org:10.1016/j.cub.2023.05.020
635 25 Karcz, S. R., Herrmann, V. R., Trottein, F. & Cowman, A. F. Cloning and characterization
636 of the vacuolar ATPase B subunit from Plasmodium falciparum. *Mol Biochem Parasitol*
637 **65**, 123-133 (1994). https://doi.org:10.1016/0166-6851(94)90121-x
638 26 Hayashi, M. *et al.* Vacuolar H(+)-ATPase localized in plasma membranes of malaria
639 parasite cells, Plasmodium falciparum, is involved in regional acidification of parasitized
640 erythrocytes. *J Biol Chem* **275**, 34353-34358 (2000).
641 https://doi.org:10.1074/jbc.M003323200
642 27 Marchesini, N., Vieira, M., Luo, S., Moreno, S. N. & Docampo, R. A malaria parasite-
643 encoded vacuolar H(+)-ATPase is targeted to the host erythrocyte. *J Biol Chem* **280**,
644 36841-36847 (2005). https://doi.org:10.1074/jbc.M507727200
645 28 Rajaram, K., Liu, H. B. & Prigge, S. T. Redesigned TetR-Aptamer System To Control
646 Gene Expression in Plasmodium falciparum. *mSphere* **5** (2020).
647 https://doi.org:10.1128/mSphere.00457-20
648 29 Ganesan, S. M., Falla, A., Goldfless, S. J., Nasamu, A. S. & Niles, J. C. Synthetic RNA-
649 protein modules integrated with native translation mechanisms to control gene
650 expression in malaria parasites. *Nat Commun* **7**, 10727 (2016).
651 https://doi.org:10.1038/ncomms10727
652 30 Wagner, J. C., Platt, R. J., Goldfless, S. J., Zhang, F. & Niles, J. C. Efficient CRISPR-
653 Cas9-mediated genome editing in Plasmodium falciparum. *Nat Methods* **11**, 915-918
654 (2014). https://doi.org:10.1038/nmeth.3063
655 31 Ghorbal, M. *et al.* Genome editing in the human malaria parasite Plasmodium falciparum
656 using the CRISPR-Cas9 system. *Nat Biotechnol* **32**, 819-821 (2014).
657 https://doi.org:10.1038/nbt.2925
658 32 Ho, C. M. *et al.* Malaria parasite translocon structure and mechanism of effector export.
659 *Nature* **561**, 70-75 (2018). https://doi.org:10.1038/s41586-018-0469-4
660 33 Ressurreicao, M. *et al.* Use of a highly specific kinase inhibitor for rapid, simple and
661 precise synchronization of Plasmodium falciparum and Plasmodium knowlesi asexual
662 blood-stage parasites. *PLoS One* **15**, e0235798 (2020).
663 https://doi.org:10.1371/journal.pone.0235798
664 34 Krugliak, M., Zhang, J. & Ginsburg, H. Intraerythrocytic Plasmodium falciparum utilizes
665 only a fraction of the amino acids derived from the digestion of host cell cytosol for the
666 biosynthesis of its proteins. *Mol Biochem Parasitol* **119**, 249-256 (2002).
667 https://doi.org:10.1016/s0166-6851(01)00427-3

35 Goldberg, D. E. Hemoglobin degradation in Plasmodium-infected red blood cells. *Semin Cell Biol* **4**, 355-361 (1993). https://doi.org:10.1006/scel.1993.1042

36 Spielmann, T., Gras, S., Sabitzki, R. & Meissner, M. Endocytosis in Plasmodium and Toxoplasma Parasites. *Trends Parasitol* **36**, 520-532 (2020). https://doi.org:10.1016/j.pt.2020.03.010

37 Jonscher, E. *et al.* PfVPS45 Is Required for Host Cell Cytosol Uptake by Malaria Blood Stage Parasites. *Cell Host Microbe* **25**, 166-173 e165 (2019). https://doi.org:10.1016/j.chom.2018.11.010

38 Milani, K. J., Schneider, T. G. & Taraschi, T. F. Defining the morphology and mechanism of the hemoglobin transport pathway in Plasmodium falciparum-infected erythrocytes. *Eukaryot Cell* **14**, 415-426 (2015). https://doi.org:10.1128/EC.00267-14

39 Wang, R. *et al.* Molecular basis of V-ATPase inhibition by bafilomycin A1. *Nature Communications* **12**, 1782 (2021). https://doi.org:10.1038/s41467-021-22111-5

40 Parra, K. J. & Kane, P. M. Reversible association between the V1 and V0 domains of yeast vacuolar H+-ATPase is an unconventional glucose-induced effect. *Mol Cell Biol* **18**, 7064-7074 (1998). https://doi.org:10.1128/MCB.18.12.7064

41 Parra, K. J., Keenan, K. L. & Kane, P. M. The H subunit (Vma13p) of the yeast V-ATPase inhibits the ATPase activity of cytosolic V1 complexes. *J Biol Chem* **275**, 21761-21767 (2000). https://doi.org:10.1074/jbc.M002305200

42 Stasic, A. J. *et al.* The Toxoplasma Vacuolar H(+)-ATPase Regulates Intracellular pH and Impacts the Maturation of Essential Secretory Proteins. *Cell Rep* **27**, 2132-2146 e2137 (2019). https://doi.org:10.1016/j.celrep.2019.04.038

43 Francis, S. E., Sullivan, D. J., Jr. & Goldberg, D. E. Hemoglobin metabolism in the malaria parasite Plasmodium falciparum. *Annu Rev Microbiol* **51**, 97-123 (1997). https://doi.org:10.1146/annurev.micro.51.1.97

44 Liu, J., Istvan, E. S., Gluzman, I. Y., Gross, J. & Goldberg, D. E. Plasmodium falciparum ensures its amino acid supply with multiple acquisition pathways and redundant proteolytic enzyme systems. *Proc Natl Acad Sci U S A* **103**, 8840-8845 (2006). https://doi.org:10.1073/pnas.0601876103

45 Ludwig, J. *et al.* Identification and characterization of a novel 9.2-kDa membrane sector-associated protein of vacuolar proton-ATPase from chromaffin granules. *J Biol Chem* **273**, 10939-10947 (1998). https://doi.org:10.1074/jbc.273.18.10939

46 Alder, A. *et al.* The role of Plasmodium V-ATPase in vacuolar physiology and antimalarial drug uptake. *Proc Natl Acad Sci U S A* **120**, e2306420120 (2023). https://doi.org:10.1073/pnas.2306420120

47 Hameed, P. S. *et al.* Triaminopyrimidine is a fast-killing and long-acting antimalarial clinical candidate. *Nat Commun* **6**, 6715 (2015). https://doi.org:10.1038/ncomms7715

48 Reader, J. *et al.* Multistage and transmission-blocking targeted antimalarials discovered from the open-source MMV Pandemic Response Box. *Nat Commun* **12**, 269 (2021). https://doi.org:10.1038/s41467-020-20629-8

49 Meibalan, E. *et al.* Host erythrocyte environment influences the localization of exported protein 2, an essential component of the Plasmodium translocon. *Eukaryot Cell* **14**, 371-384 (2015). https://doi.org:10.1128/EC.00228-14

50 Ling, L. *et al.* Genetic ablation of the mitoribosome in the malaria parasite Plasmodium falciparum sensitizes it to antimalarials that target mitochondrial functions. *J Biol Chem* **295**, 7235-7248 (2020). https://doi.org:10.1074/jbc.RA120.012646

51 Ke, H., Dass, S., Morrisey, J. M., Mather, M. W. & Vaidya, A. B. The mitochondrial ribosomal protein L13 is critical for the structural and functional integrity of the mitochondrion in Plasmodium falciparum. *J Biol Chem* **293**, 8128-8137 (2018). https://doi.org:10.1074/jbc.RA118.002552

A

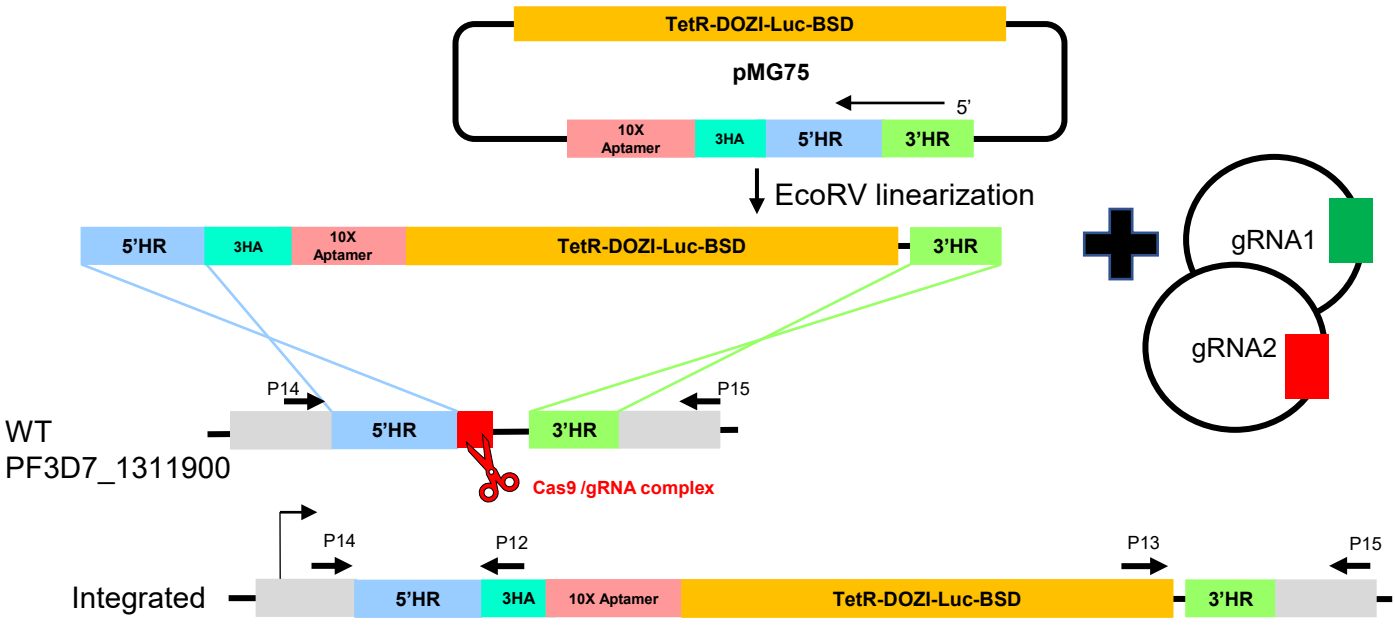

B

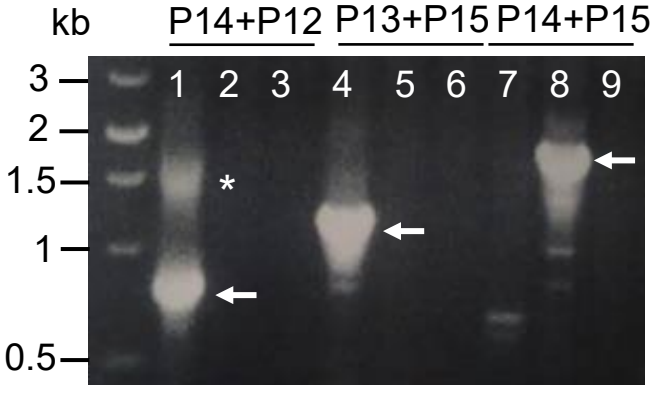

Lanes 1, 4, 7: V_1A transgenic DNA
Lanes 2, 5, 8: WT DNA
Lanes 3, 6, 9: No DNA controls

C

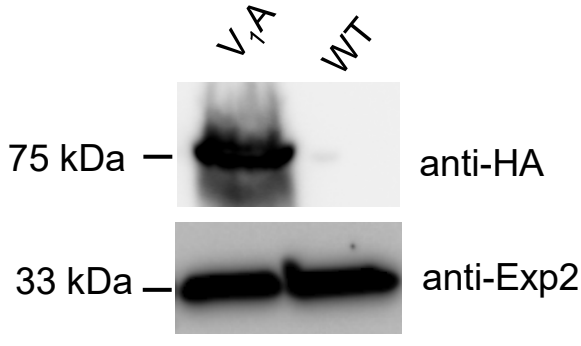

Figure 1. Endogenous tagging of V_1A via CRISPR/Cas9 for conditional expression

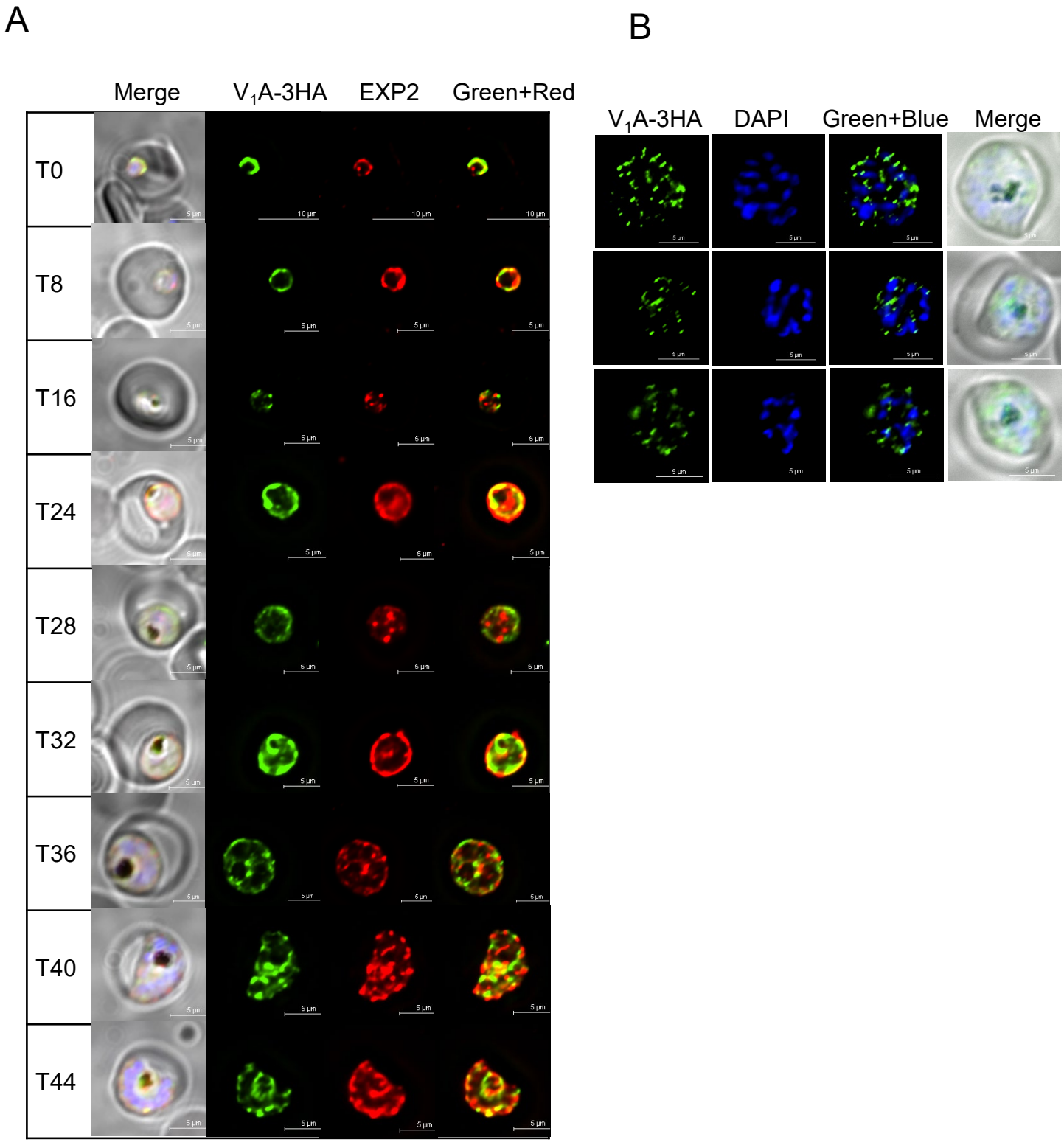

Figure 2. Localization of V_1A throughout the asexual blood stages

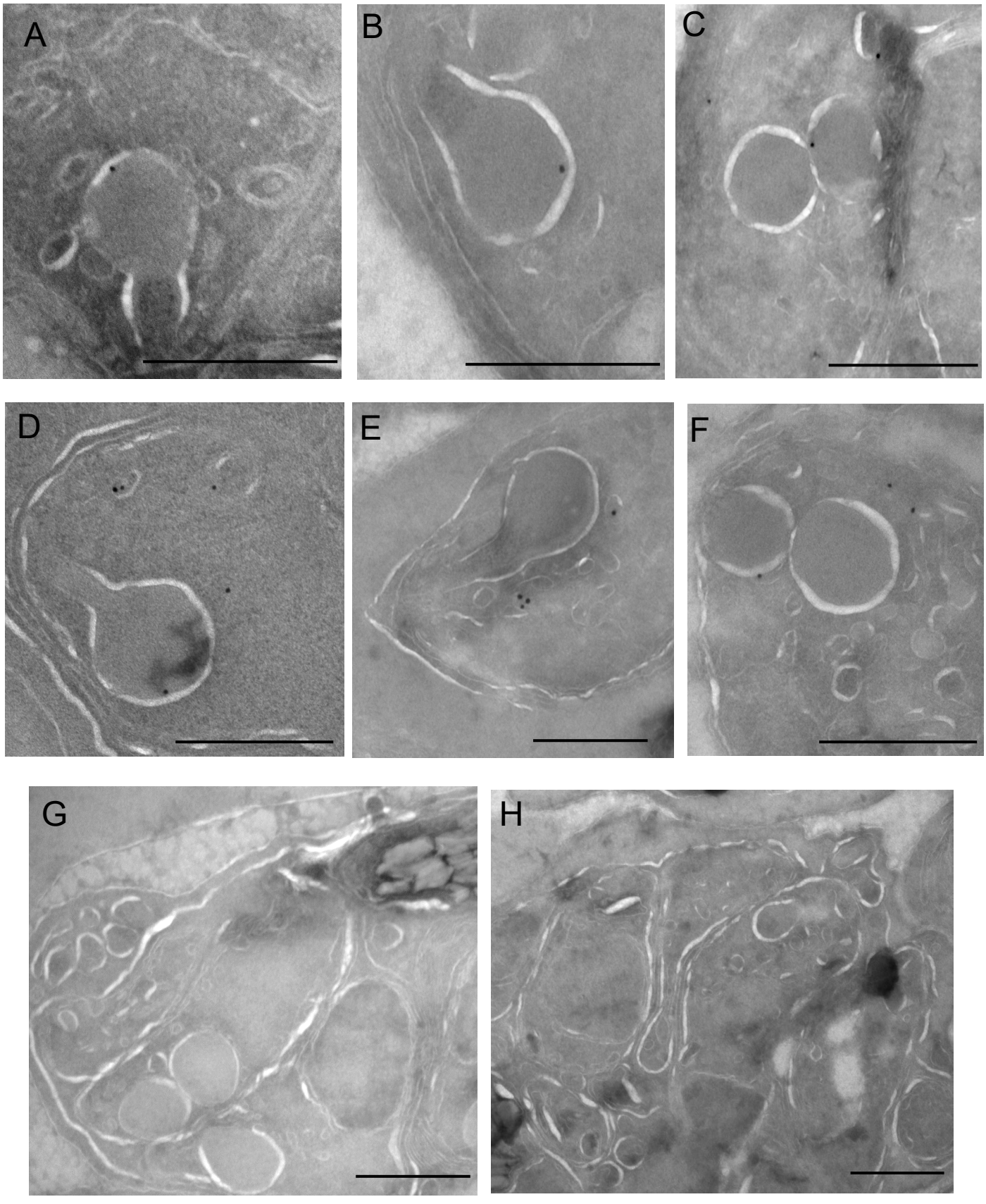

Figure 3. Localization of V_1A on the secretory organelles in mature schizont stage parasites

A

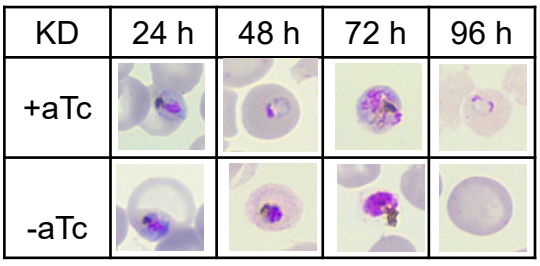

B

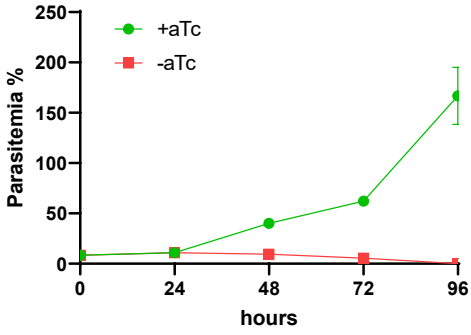

C

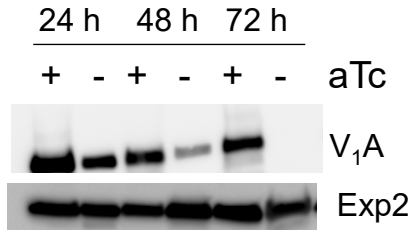

D

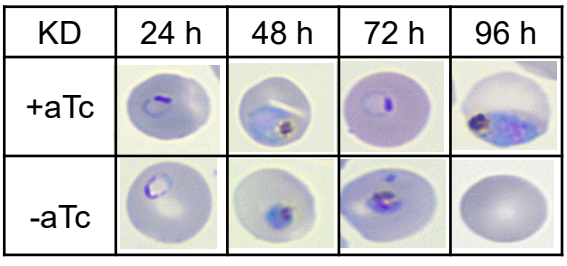

E

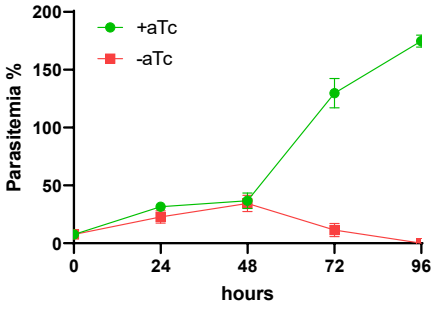

F

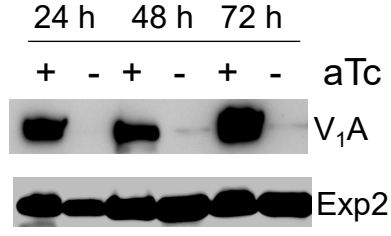

G

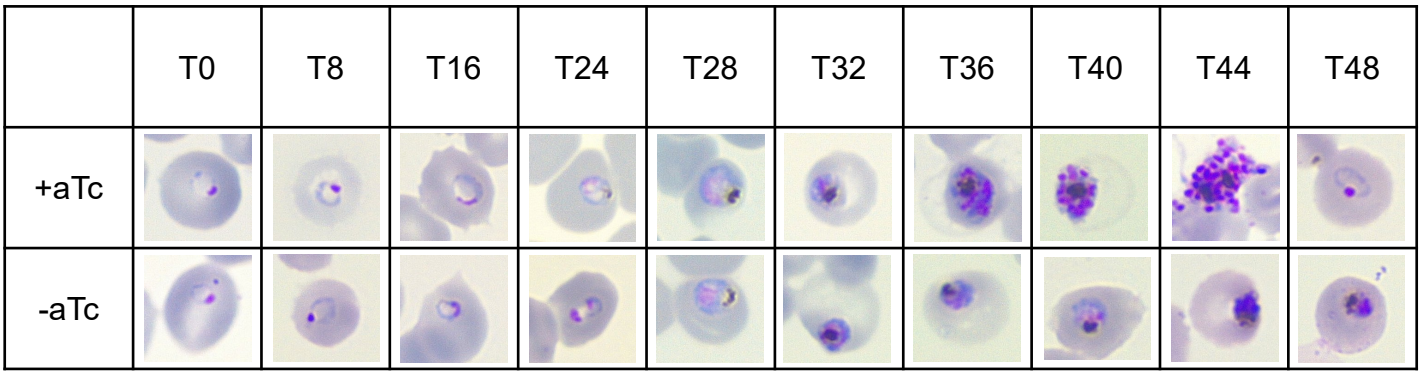

Figure 4. Essentiality of V-type ATPase in the asexual blood stages

A

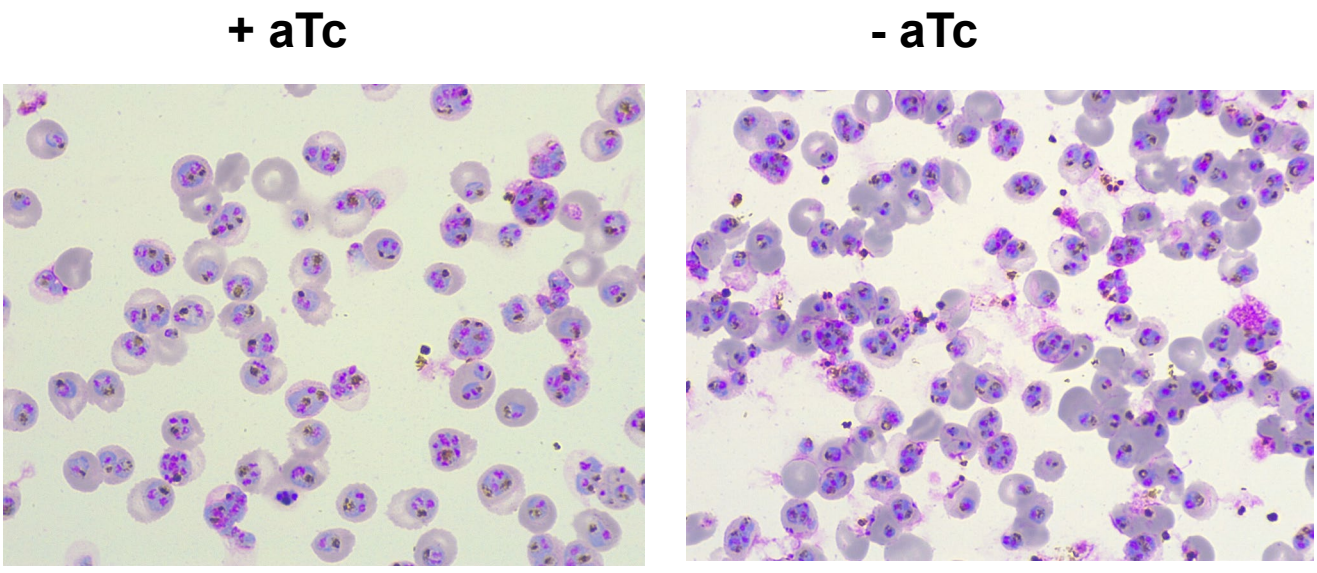

B

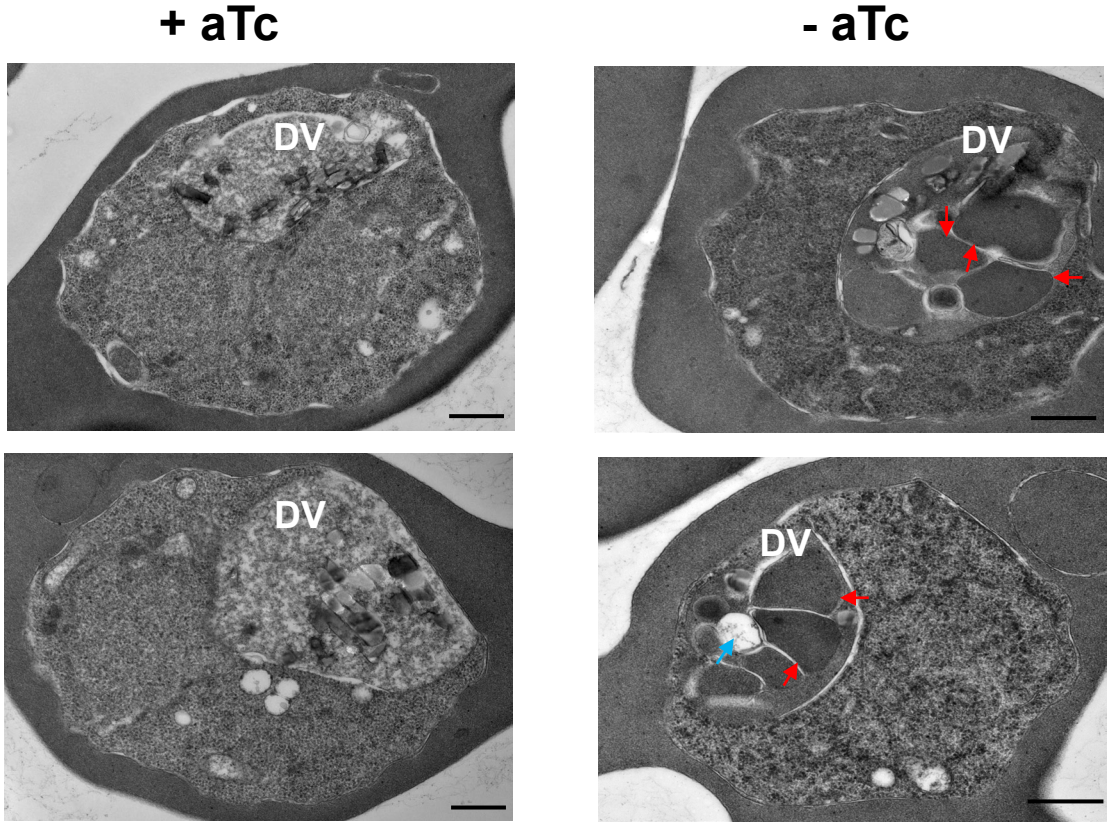

Figure 5. V-type ATPase is essential for hemoglobin digestion in the digestive vacuole

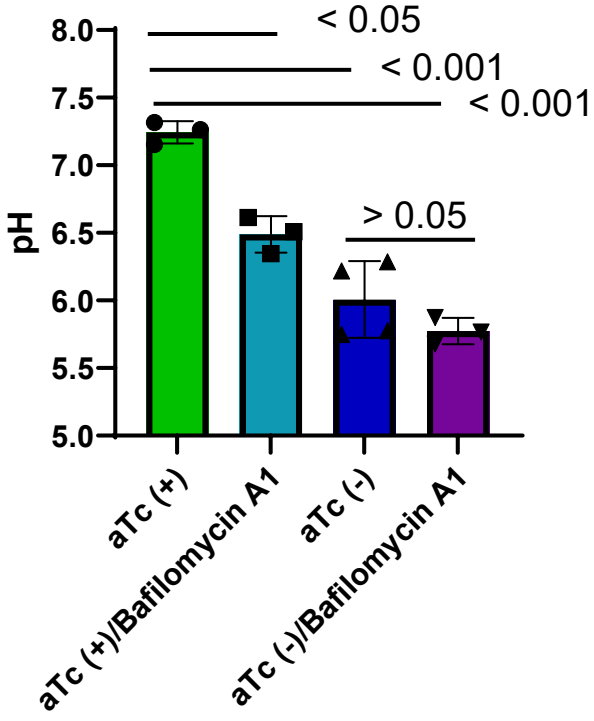

Figure 6. V-type ATPase regulates cytosolic pH in trophozoite stage parasites

A

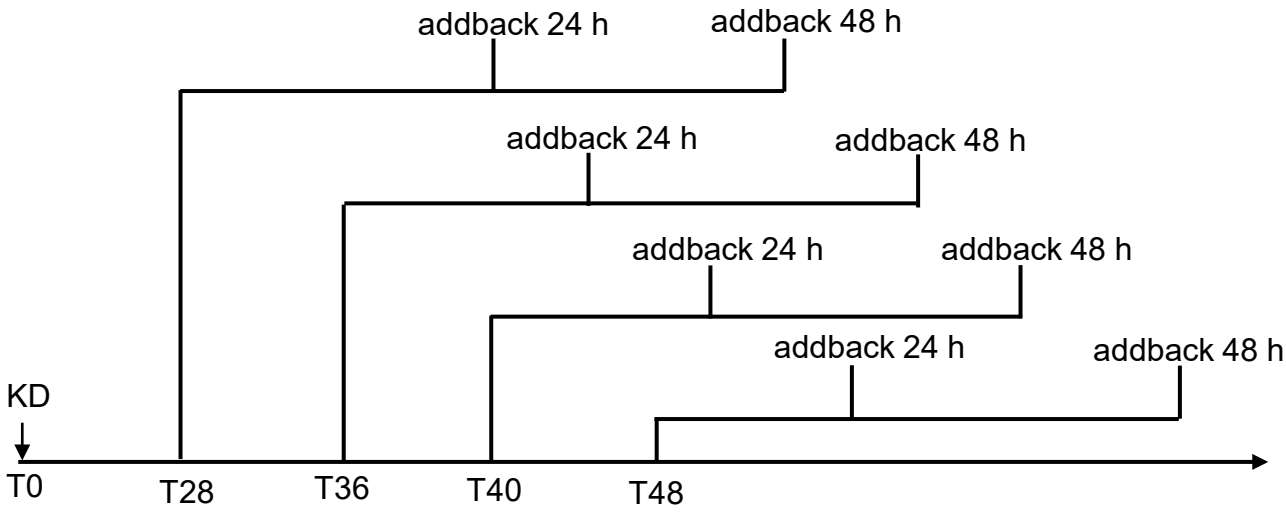

B

	+aTc	-aTc	addback 24 h	addback 48 h
KD 28 h				
KD 36 h				
KD 40 h				
KD 48 h				

Figure 7. Viability of the V-type ATPase knockdown parasites

A

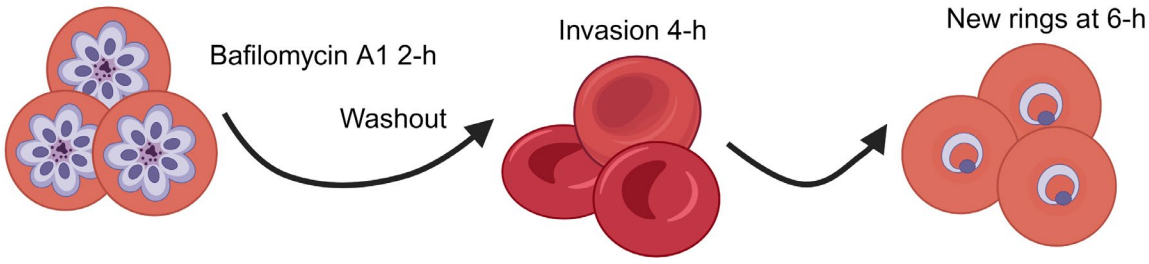

B

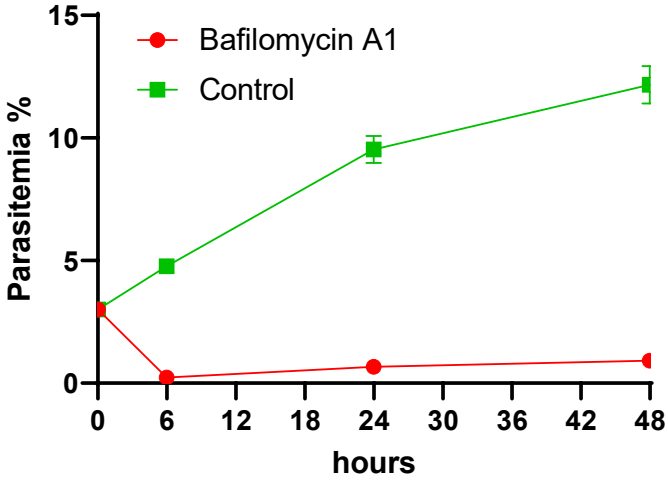

C

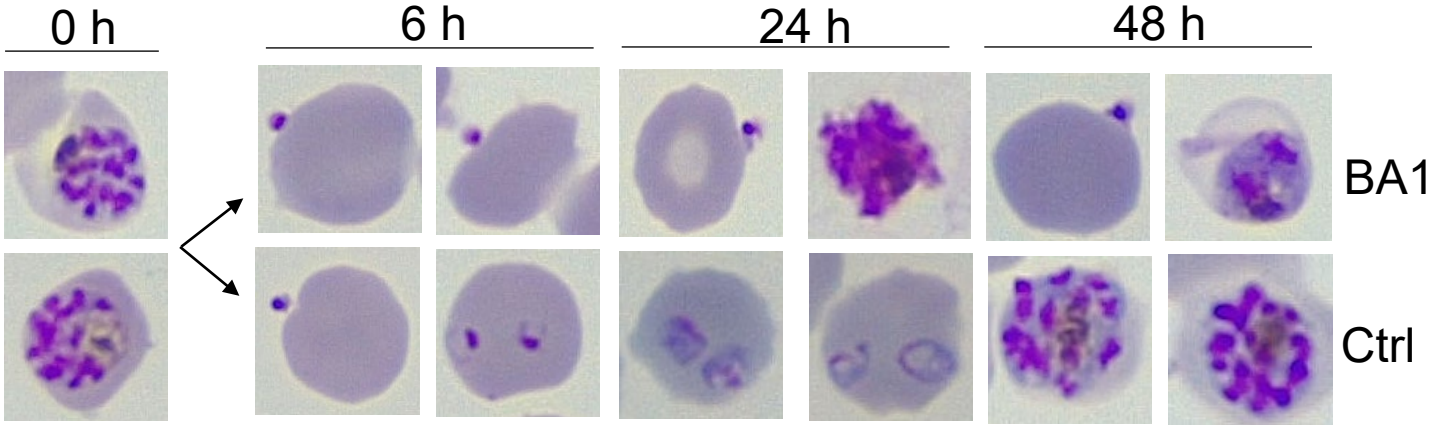

Figure 8. Effects of Bafilomycin A1 on parasite egress and invasion

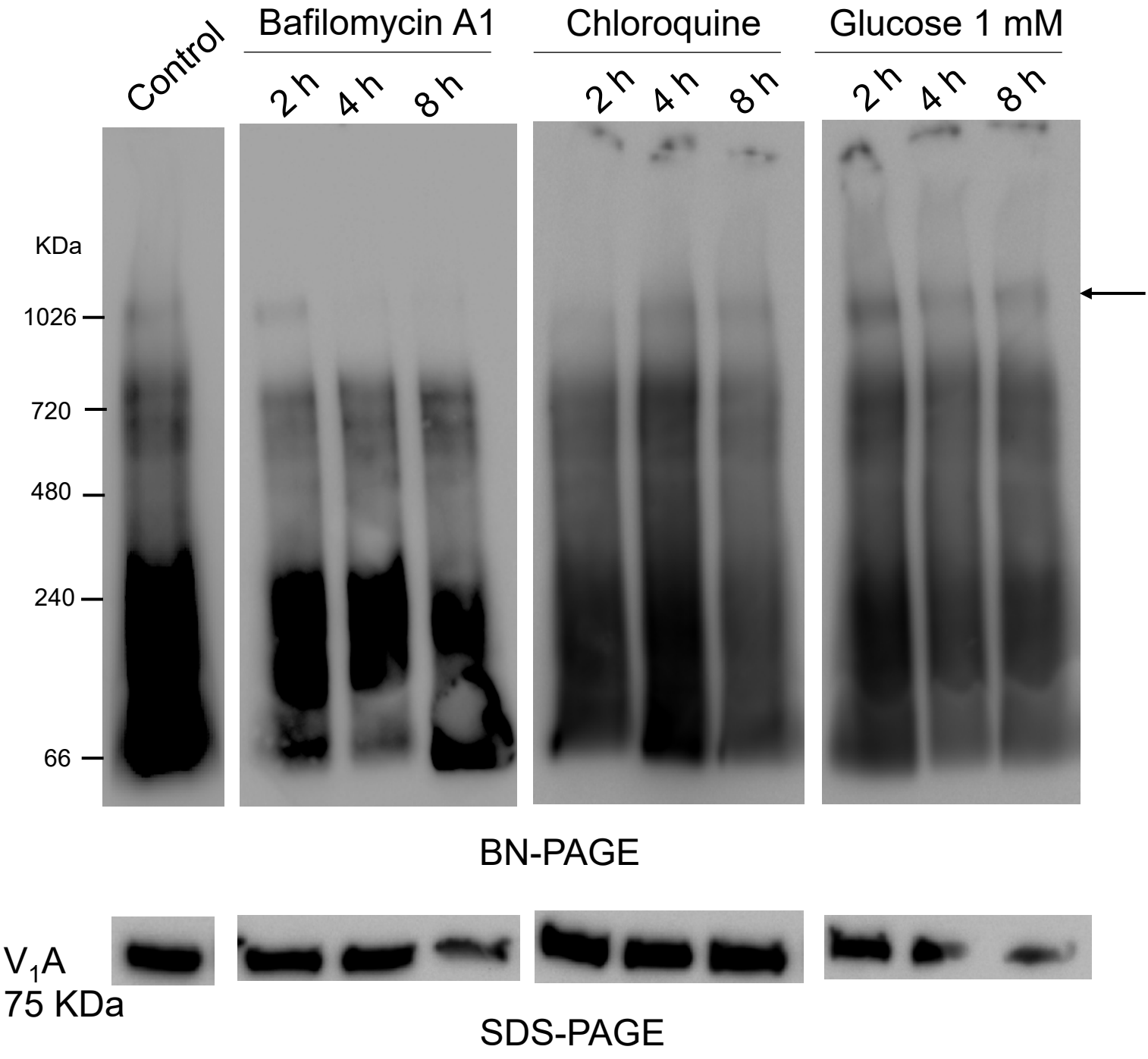

Figure 9. The stability of V-type ATPase complex under various conditions